Operability of District Heating Plants combining a Large-Scale Solar Thermal Field with Condensing Wood Chip Boilers – A Case Study in Switzerland

Xavier Jobard[1] and Alexis Duret[1]

[1] Laboratory for Solar Energy and Building Physics
School of Management and Engineering Vaud, HES-SO, Yverdon-les-Bains (Switzerland)

Abstract

The subject of this work is the integration and operability of a large-scale solar thermal field with condensing wood chip boilers for district heating application in rural areas. Based on a case study in Switzerland, a large-scale solar field is designed to be coupled with the existing heating plant composed of two wood boilers with external flue gas condensers. The operability of the new central heating plant is then assessed with numerical simulations carried out with TRNSYS. In a first step, two scenarios with two different solar fractions are simulated to analyze the performances of the solar system and the influence of the integration of the solar thermal field on the operation of the wood boilers. The main results are: 1) The specific productivity is between 450 and 500 $kWh.m^{-2}.y^{-1}$ for the considered operating temperatures and solar fractions. 2) The startup cycles are important if the heating needs in summer are not totally covered by the solar system. 3) After optimization of the controls, the startup cycles of the boilers in mid-season are very low.

Keywords: Solar District Heating, Large-scale solar thermal, Wood Chip Boiler, Numerical simulation, operability

1. Introduction

The subject of the proposed article is the integration of large scale solar thermal field with biomass boilers for district heating (DH) application in rural areas. (Lund et al., 2014) identifies this combination as relevant to the principle of 4th Generation DH principles assisting the development of sustainable energy systems. Moreover, (Tschopp et al., 2020) refers to installations on this best practice concept as "Bioenergy Villages" and report on the first demonstration object in Büsingen, DE. There a solar field is coupled with two wood chip boilers backed-up with an oil boiler. The solar field shows good performance with 13% of solar fraction (100% from end of June to mid-August) and with a solar specific productivity of 603 $kWh.m^{-2}.y^{-1}$. Based on this success, five similar plants were commissioned in 2018. However, no information was found on the operability of these plants and the impact on the startup's cycles of the boilers. Only (Ruesch, 2020) through numerical simulation concluded that the starts up cycles of wood boilers can be important in summer and widely reduced with the integration of solar heat production. However, increase of the boiler's startups was also found in mid-season but only marginally higher. In a similar way, this paper proposes to study the operability of central heating plant combining a large-scale solar thermal field and wood chip boilers supplying a DH network. The particularity is that the boilers are equipped with flue gas condensers and induce higher complexity to integrate the solar thermal system.

Base on a case study located in Switzerland with extensive monitoring data, numerical simulations were carried out at a fine timestamp allowing the evaluation of the operability of the system. The modeled central heating plant consists of the actual installed condensing wood chip boilers upgraded with a large scale solar thermal field and thermal energy storage (TES). Firstly, the actual design of the heating plant and the selected solar thermal field integration concept will be described. Secondly, chosen numerical modeling method and models are presented briefly before finally discussing the simulation results.

doi:10.18086/eurosun.2022.04.03 Available at http://proceedings.ises.org

2. DH plant and integration of solar thermal field with TES

The considered DH network is located in the rural town of Les Ponts-de-Martel, NE, Switzerland and went into operation in September 2007. Initially, 32 buildings were supplied by the network, with a total length of 2.1 km. Ten years later, nearly 80 buildings are connected to the district heating system. The entire district heating network belongs to a cooperative called "Le Marais-rouge". Each consumer (including potential future consumers) of the network can be part of this company. This particular legal status makes "Le Marais-rouge " a completely different DH system than the one managed by utility companies. The involvement of the consumers in a cooperative makes it easier to access the secondary heat distribution circuits for energy efficiency measures, since the heat consumers benefit from them: the price of the energy consumed depends on the overall efficiency of the district heating network. Therefore and thanks to efficient substation design, very low return temperatures are achieved with a yearly mean value in 2019 of 44°C and peak value as low as 28°C were measured in winter. Table 1 presents the main characteristic of the DH network “le Marais-Rouge”.

Tab. 1: Characteristic of the district heating network of “les Marais-Rouge”, values given for the year 2019

Heat supply	5.81	GWh
Linear heat density	1.53	$MWh.kml^{-1}.y^{-1}$
Heat losses	0.76	GWh
Supply temperatures	80 - 70	°C
Mean return temperature	44	°C

The DH network “le Marais-Rouge » makes a good candidate for the integration of solar heat: 1) its rural area provides plenty land space for the solar field, 2) low supply and return temperature allow efficient heat production and 3) main fuel should be spared for use in Winter. Only drawback found is a low heat consumption in summer causing high distribution losses. Figure 1 shows the simplified hydraulic diagram of the central heating plan comprising of 2 wood boilers (1.25 MW and 1 MW) equipped of flue gas condensers installed separately upstream of the boilers on the DH return pipe. Cascading of the boilers is possible in series in winter, while only one boiler is operated in mid-season and summer. The flue gas condensers allow to preheat the water of the network returning to the power plant. This is beneficial since it allows the recovery of energy otherwise lost in the flue gas and limits the recirculation of water in the wood-fired boilers, which must not have inlet temperatures below 65°C.

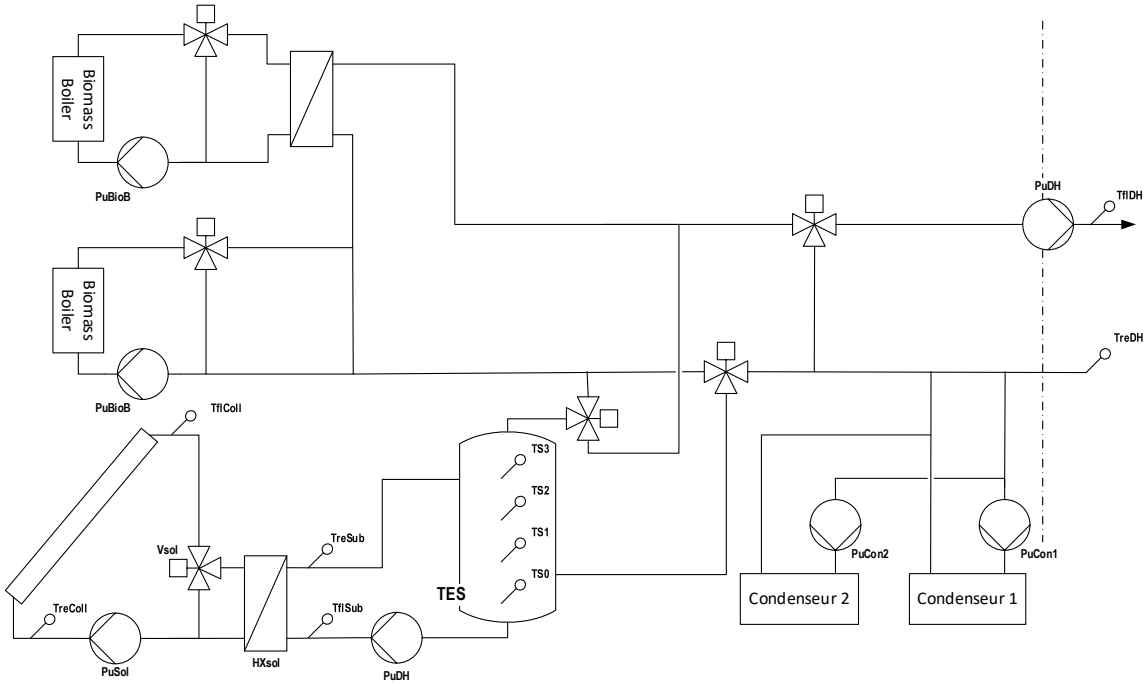

Fig. 1: Simplified hydraulic diagram of the central heating plant of the DH “le Marais-Rouge” upgraded with the integration of a large-scale solar thermal system.

The fact that the condensers need low inlet temperatures to recover effectively the latent heat contained in the flue gas, implies that the solar installation should be integrated after them. In winter and mid-season, the solar field is design to preheat the flow on the return line of the boilers. As the inlet temperature of the wood boiler should be kept above 65°C, the solar thermal system operates thus between the supply temperature of the condensers and 65°C. In summer the solar field is designed to supply, when possible, the total heat demand of the network, if not one boiler is fired-up and takes over. In winter and mid-season, the solar field inject the heat on the return line before the gas In order to guarantee the heat supply even at night or when the weather does not allow the solar installation to fulfill the demand, a hot water tank is installed to store the produced solar energy and to inject it later on the grid. The technology chosen here is insulated steel tanks. These tanks must be highly insulated. As reported (Sveinbjörnsson et al., 2017): In Denmark, those tanks are insulated with between 30 and 45 cm of mineral wool to have acceptable losses at about 2% per week for 500 m3 and 1% per week for 5000 m3 tanks. The tank is integrated in the hydraulic diagram to store exclusively solar heat. This was chosen to simplify the controls.

3. Numerical model of the system

The heating plant modeling was performed with TRNSYS 17 software (Klein and Al., 2014). The wood boilers are modeled with the type 869 developed by (Haller et al., 2011). It is a numerical model to simulate any kind of boiler of different technology and fuel and especially wood chips boilers. The parameters are defined from the data provided by the manufacturer and hourly monitoring data from the heating plant. For simplicity, the condensers are modeled with a simple model derived from the available measurements. Finally, the TES and solar field are modelled with well-known models respectively type 60 and type 832 (Haller et al., 2013). Other components (tubes, controls) are modelled with standard types from the TRNSYS library.

Validation of the models (boiler and condenser) has been conducted by comparing monitoring data with the simulation results and by assessing cvRMSE (eq. 1). Only the heat flow rates were compared with each other.

$$cvRMSE = \frac{\sqrt{\sum(y-\hat{y})^2}}{\bar{y}} \quad \text{(eq. 1)}$$

With: y the monitoring values and $\hat{y}$ the simulated values et $\bar{y}$ the average of the monitoring values.

3.1 Wood chip boiler model

The validation of the simulations gives mitigated results (see figure 2). The comparison shows high cvRMSE values (38% and 39%). The dynamic behavior of the boilers is relatively well represented considering the input data and the noise of the measurements. Indeed, the temperature measured at the boiler outlet deviates strongly from the setpoint temperature given by the water law.

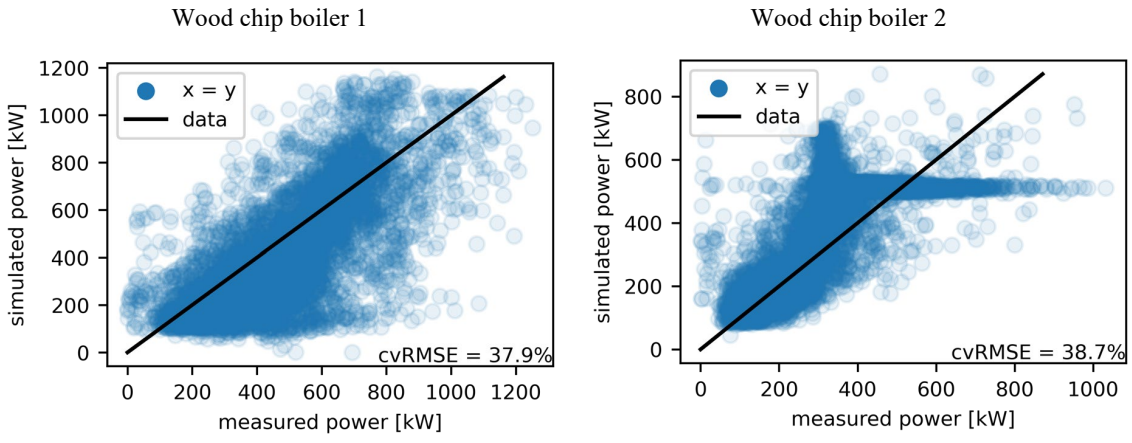

Fig. 1: Comparison of monitoring data and simulations for wood boiler 1 (left) and 2 (right)

This is confirmed by the comparison of the boiler power monotones presented at figure 3 and figure 4. Nevertheless, a reservation can be made for boiler 2 whose model does not allow to reproduce its load rate measured during the cascade operation i.e., in winter period. In fact, and as shown in the figure 4, the simulated load of boiler 2 have a level at 500 kW which does not exist. This point should be further studied to find its causes. Annually, the absolute error on the produced energy is -12% for boiler 1 and 18% for boiler 2.

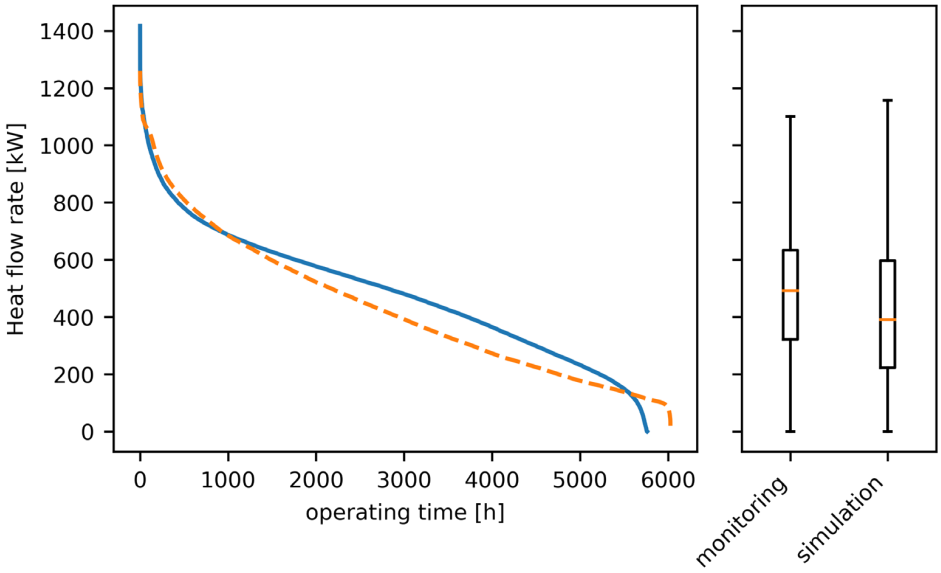

Fig. 2: Comparison of the power monotones of Boiler 1 from monitoring and simulations

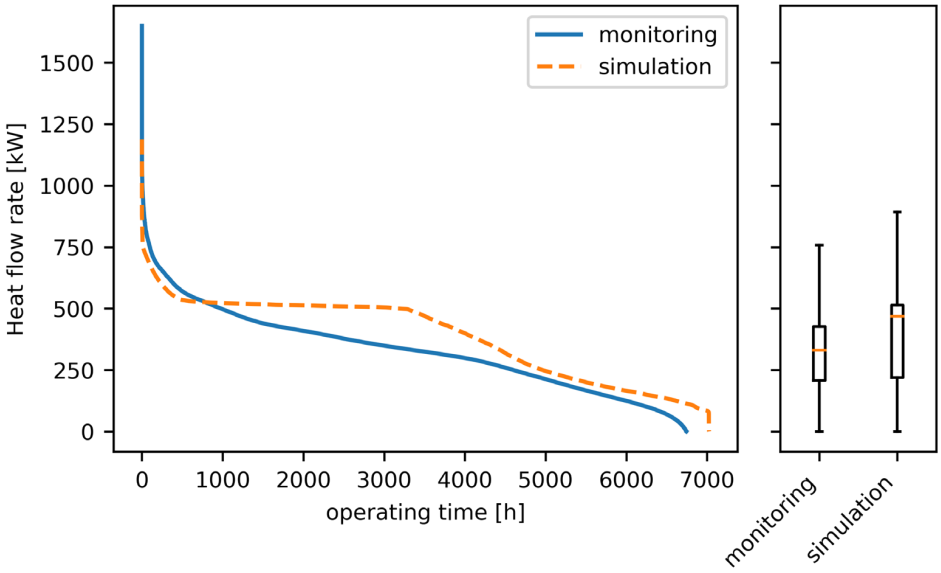

Fig. 3: Comparison of the power monotones of Boiler 2 from monitoring and simulations

3.2 Flue gas condensers

The condensers are modeled very simply by taking constant heat losses and heat recovery efficiency on the fatal heat (latent and sensible) of the flue gas at the exit of the wood boilers. The equation defining this operation is given below in equation 2:

$$\dot{Q}_{con} = \eta_{fg} \cdot (\dot{Q}_{fg} - \dot{Q}_{fg,loss}) \quad \text{(eq. 2)}$$

With :

- η_{fg}: The efficiency of heat recovery from the flue gases
- $\dot{Q}_{fg}$: The latent and sensible heat flow rate in the flue gas, given by the model of the wood boiler and the characteristics of the fuel.
- $\dot{Q}_{fg,loss}$: The sensible heat flow rate lost between the boiler and the condensers

The parameters of the equations η_{fg} and $Q_{fg,loss}$ were identified graphically by comparing the monitoring data and the result of the simulations. The values obtained are given in table 2.

Tab. 2: Parameters for the numerical condenser model

Parameters	Condenser 1	Condenser 2
$\boldsymbol{\eta_{fg}}$	0.90	0.90
$\boldsymbol{\dot{Q}_{fg,loss}}$	90 000 kJ/h	72 000 kJ/h

The figure 5 present a comparison of the results of the numerical model with the monitoring data. The graphs show that the model approximations roughly reproduce the condenser operation with a cvRMSE value of 49% for condenser 1 and 37% for condenser 2. However, the relative deviations of the annual heat production of the condensers are 30% for condenser 1 and 1% for condenser 2. The measured data show a non-linearity between the boiler heat output and the condenser heat output that the model does not reproduce. A variable efficiency and a better identification of the parameters would improve the performance of the model. However, for the purpose of this study, the model is considered satisfactory.

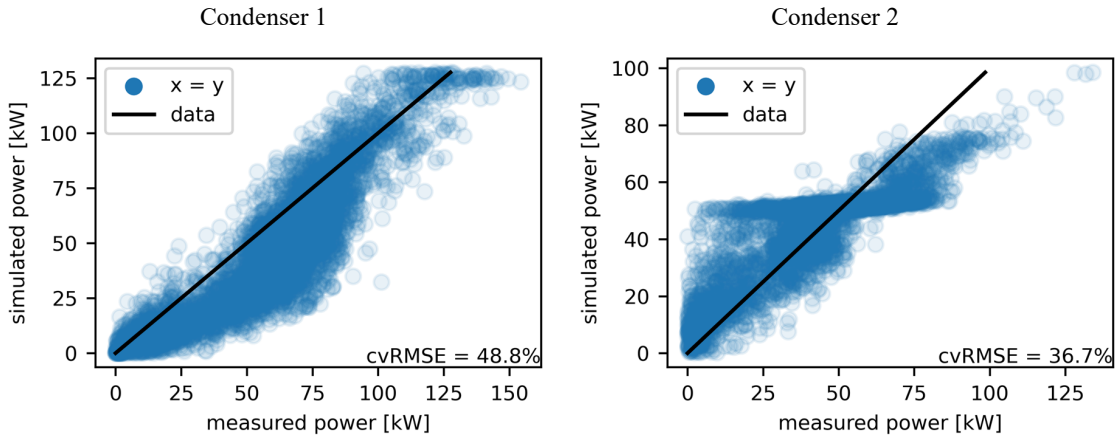

Fig. 5: Comparison of monitoring data and simulations for condenser 1 (left) and 2 (right)

3.3 Thermal Energy Storage (TES)

The hot water tank is modelled with the generic type 60. It is configured to have two double ports, on for charging the tank with solar heat and one to discharge the tank. Type 60 takes as main parameters, the tank's volume VS, height H, and overall heat loss coefficient U. To vary the volume of the tank, height/diameter ratio has been fixed to 2 to ensure compactness while keeping an efficient stratification. The overall heat loss coefficient has been calculated for 5 different volumes [50, 500, 5000, 10000, 15000] m^3. The calculation was carried according to (Bergman and Incropera, 2011) with a outer convection heat transfer coefficient of 10 W/(m^2.K), insulation thickness of 0.45 m, heat conductivity of 0.04 W/(m.K) and assuming constant physical properties of material over the temperature range (20°C – 100°C). The results were regressed to obtain a continuous function given in equation 3 and figure 6:

$$U = 0.11\,.\,(VS - 48)^{-0.02}; r^2 = 0.998 \qquad \text{(eq. 3)}$$

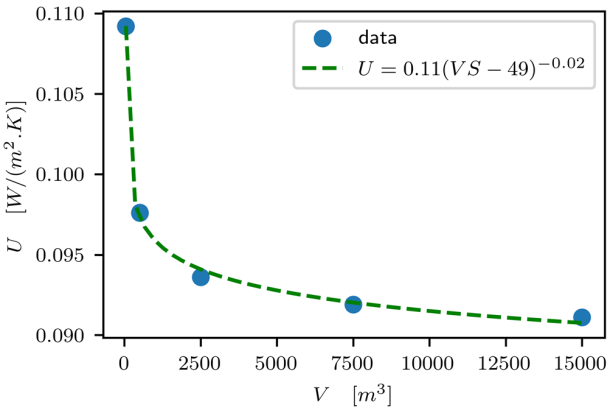

Fig. 4: Evolution of the heat loss coefficient U as a function of the volume of the storage tank with a constant height/diameter ratio of 2.

3.4 Solar collectors

The solar collectors are modelled with a well-known third-party model, type 832. The performance coefficients considered are given in table 3, they were obtained by averaging the coefficients of large flat plate collector on the market these last years from several European manufacturers. Heat capacity and incident angle modifier coefficient for diffuse and direct irradiation are also taken into account.

Tab. 3 : Performance coefficient of an average large scale flat collector

	value	**unit**
$\boldsymbol{\eta_0}$	0.79	-
$\boldsymbol{a_1}$	2.9	W/(m^2.K)
$\boldsymbol{a_2}$	0.0135	W/(m^2.K^2)

4. Results

This section presents the results obtained with the numerical model described in section 3. and their analysis to show the technical potential of integrating solar thermal in wood based and rural DH network. An underlying objective is to give elements on the influence of the solar thermal installation on the operation of the wood chip boilers and to establish if there is an increase of the boiler startup cycles. For this purpose, several scenarios were implemented and sized based on an available pre-feasibility study:

1. Solar fraction less than 15% with 1500 m^2 of solar thermal panels and 75 m^3 of TES (scenario 1)
2. Solar fraction around 30% with 3300 m^2 and 1060 m^3 TES (scenario 2)
3. Optimization of startup cycles for scenario 2 (scenario 3)
4. Sensitivity analysis of the sizing parameters (Gross panel area and TES size)

4.1 Scenario 1: low solar fraction

A first scenario was defined to analyze systems with a low solar fraction (< 15%) and a limited storage volume. The solar heat is injected on the return line before the boilers and downstream of the condensers. The annual results presented in table 4 shows a very satisfactory productivity and efficiency of respectively 516 kWh/(m^2.an) and 33%. The solar heat is thus very well used.

On the one hand, the figure 7 also shows a very good solar coverage above 60% in summer for the months of July and August but insufficient to cover the total needs. On the other hand, the coupling return/return generates important cycle of starting of the wood boiler in summer (figure 8). It starts every time the installation does not allow to cover the needs completely. An optimization is surely possible to reduce them, but it would not allow to totally suppress these cycles. The installation of a larger storage that can be used by the biomass boilers would be beneficial.

Tab. 4: Annual performance of the solar system including storage losses in scenario 1

Solar resource in the collector plane (30°, 0° South)	1558	kWh/(m^2 .a)
Yield	773	MWh
Productivity	516	kWh/(m^2 .a)
Solar efficiency	33	%
Solar fraction	13	%

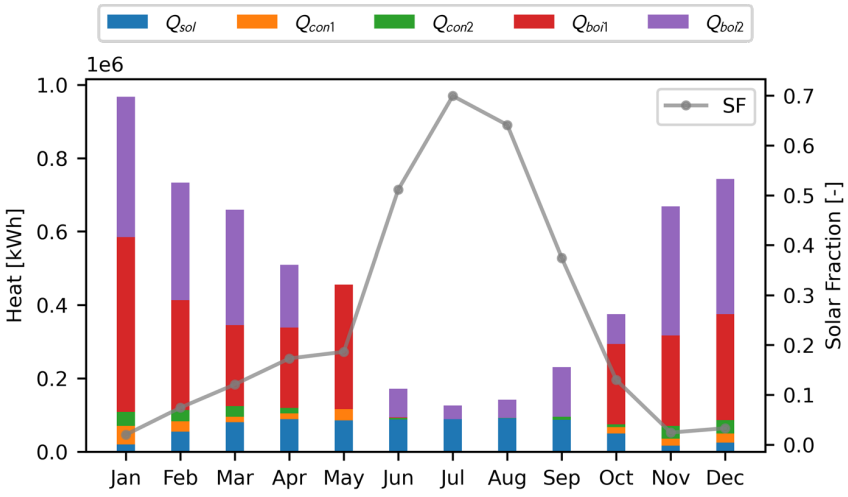

Fig. 7: Monthly heat production per installation and solar fraction for scenario 1

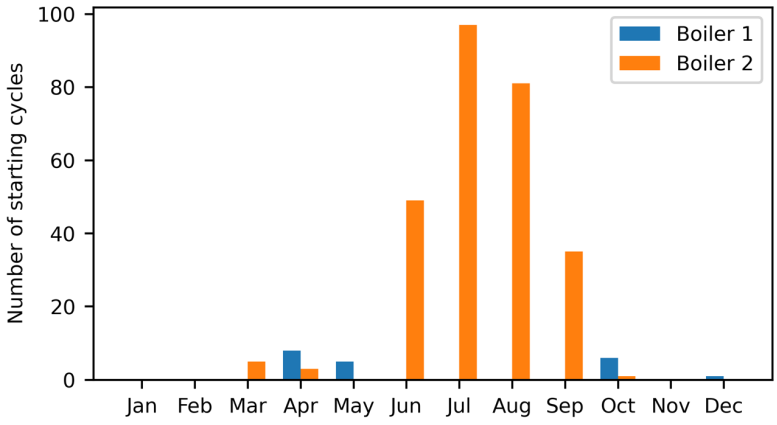

Fig. 8: Number of boiler start-up cycles with injection on the outflow in the off-season and in the summer of scenario 1

4.1 Scenario 2: Solar fraction of about 30%.

The sizing of this variant is intended to turn off the boilers during the summer period. The figure 9 shows a possible boiler shutdown from July to the end of September. The results (table 5) show an interesting productivity higher than 450 kWh/(m^2 .an) including storage loss. The yield is also in the expected range, although slightly lower than in scenario 1. As for the solar fraction, it falls short at 26% compared to the target value of 30%. The monthly results presented in figure 9 show that the fraction reaches 100% of the needs for the months of July, August, and September. In the off-season the solar fraction is also interesting between 30 and 40%. The boiler load is also reduced during these months.

Tab. 1: Annual performance of the solar system including storage losses in scenario 2

Solar resource in the collector plane (30°, 0° South)	1558	kWh/(m^2 .a)
Yield	1497	MWh
Productivity	454	kWh/(m^2 .a)
Solar efficiency	29	%
Solar fraction	25.7	%

However, this is only problematic for the month of June, as shown in figure 10. Because the solar system is very close to covering the entire demand of the DH network but does not reach it, boiler 1 presents a high number of starting cycles (n=60). This operation is not satisfactory and can strongly reduce the performance of the boiler. An optimization of the operation of the installation is therefore necessary and has been realized in scenario 3.

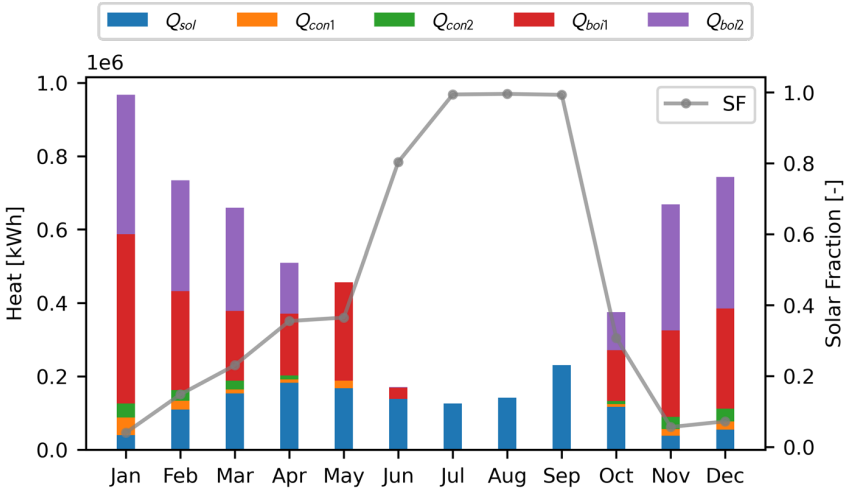

Fig. 9: Monthly heat production per installation and solar fraction for scenario 2

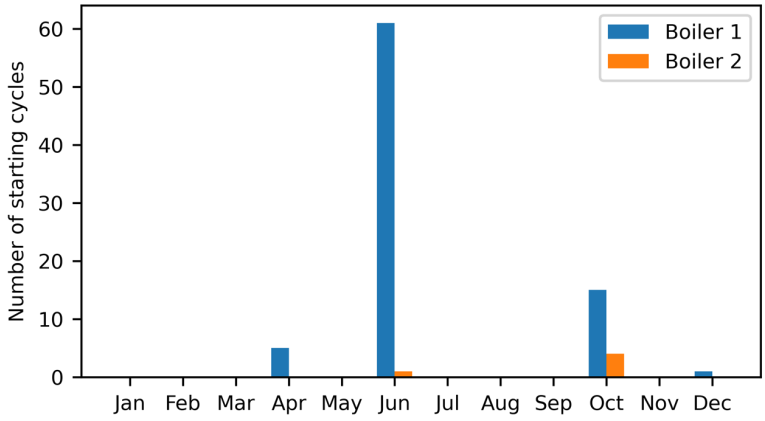

Fig. 10: Number of boiler start-up cycles with injection on the outflow in the off-season and in summer

4.3 Scenario 3: Optimization of boiler start-up cycles in the off-season

In scenario 2, boiler 1 cycles strongly in June. In this scenario, the season changes is optimized in order to shut down the boiler earlier and leave the solar thermal field to fulfill the entire demand sooner. After analyzing the instantaneous powers of the boilers, an advancement of the summer to the hour at 3634 instead of 3967 and an extension of the fall inter season to the hour 7238 instead of 7057 was implemented. The figure 11 shows a clear decrease in boiler start-up cycles.

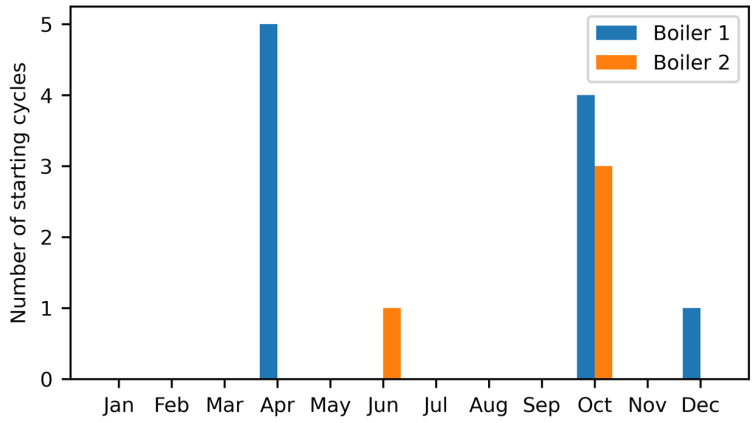

Fig. 11: Number of boiler start-up cycles with injection on the outward journey in the off-season and in the summer after optimization of the dates of the change of season

After this optimization, it also results in a better solar heat production in June and allows to cover the total heat demand of this month, see figure 12.

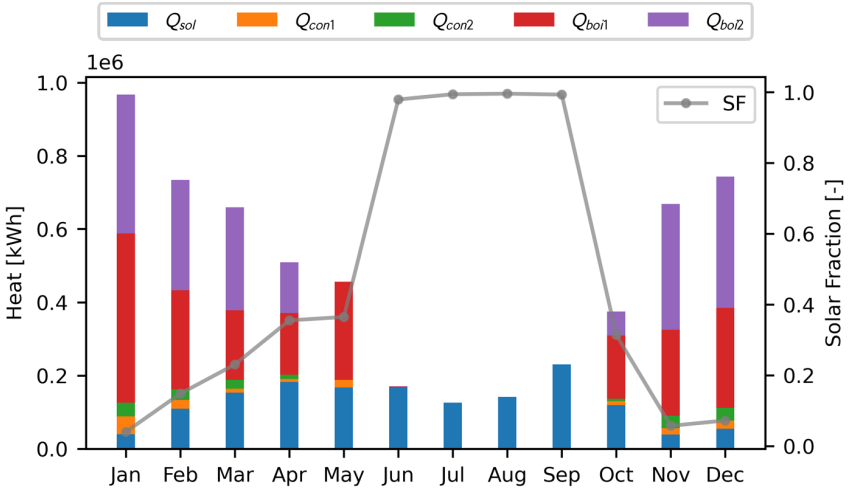

Fig. 12: Monthly heat production per installation and solar fraction for the optimized scenario 2

From the point of view of the annual performances presented in the table 6. A slight improvement is noted with a gain of 2% on the solar yield and one additional efficiency point.

Tab. 6: Annual performance of the solar system including storage losses in optimized scenario 2

Solar resource in the collector plane (30°, 0° South)	1558	kWh/(m2.a)
Yield	1531	MWh
Productivity	464	kWh/(m2.a)
Solar efficiency	30	%
Solar fraction	26.2	%

4.4 Sensitivity analysis

In order to be able to assess the sizing of the solar thermal installation and its storage, 6 sizes of solar field from 1500 m^2 to 4000 m^2 as well as 6 specific storage volumes (VS_{spe}) were simulated with the TRNSYS model described above. Figure 13 presents the results by showing the variation of the solar fraction (solid lines) in parallel with the specific productivity of the solar thermal panels (dashed lines) as a function of the installed solar panel area. Like any solar thermal system, 3 main trends are observed:

- The larger the solar field, the larger is the solar fraction.
- The larger the solar fraction, the lower is the specific productivity of the panels as the system losses increase.
- For a given solar array size, there is an optimal specific storage volume above which there is no increase in the specific productivity of the panels.

It is found that a specific volume of 0.05 [m3 /m2] is not optimal with respect to the specific productivity of the solar field. Taking 1500 m2, the increase of the specific volume from 0.05 to 0.25 [m3 /m2] allows a gain of specific productivity from 535 kWh/(m2 .an) to 600 kWh/(m2 .an) that is to say approximately 12% of increase. Beyond 0.25, the gain is no longer as decisive for this panel surface.

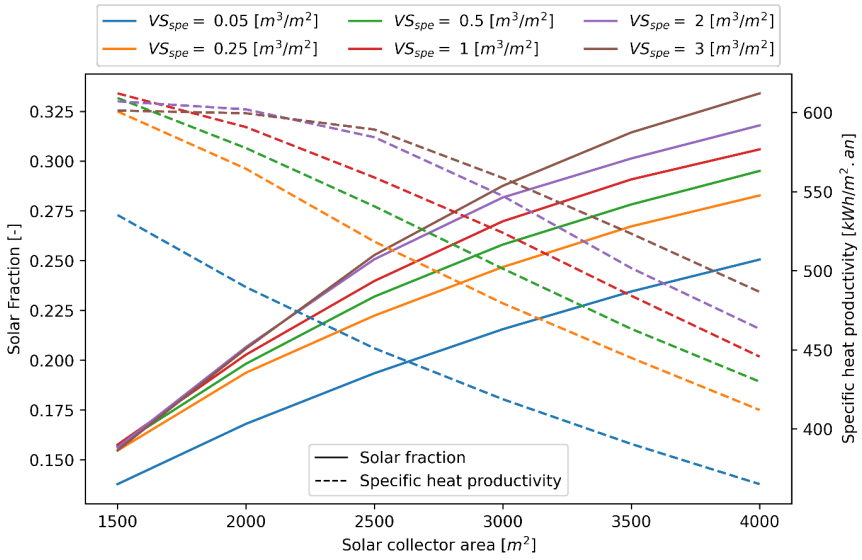

Fig. 5: Solar fraction and specific heat productivity for different surfaces of solar thermal panels connected to the Ponts-de-Martel boiler room obtained from the TRNSYS model results

5. Conclusion

A numerical model of the boiler room of the DH "les Marais-Rouge" integrating a large-scale solar thermal system was developed with the software TRNSYS 17. In a first step, this model allowed to calculate 2 scenarios of solar coverage (< 15% and about 30%) and to analyze the performances of the solar system and the influence of the integration of the solar thermal on the operation of the wood boilers. The main results are:

- The specific solar yield is between 450 and 500 kWh/(m^2 .an) for the operating temperatures and solar coverages considered
- Start-up cycles are important if the summer heat demand is not fully covered by the solar system
- Boiler start-up cycles in mid-season are very low in the scenarios studied

In a second step, a sensitivity study on the size of the field and the specific storage volume was conducted in order to better appreciate the sizing parameters. From the point of view of the specific heat productivity, an optimum storage volume appears between 0.5 m^3/m^2 and 1 m^3/m^2 for a 1500 m^2 surface of solar thermal panels. This optimum increases for larger surfaces (between 2 and 3 m^3/m^2 to 2000 m^2) to reach very large storage volumes (> 5 000 m^3). These applications are generally not very profitable in Switzerland. However, a financial calculation should be made to confirm this trend.

6. Acknowledgments

This work was financially supported, by the Swiss Federal Office of Energy. This work was carried out during the SolCAD project carried out in collaboration with the CREM, KAEMCO and Planair. The authors would also like to thank M. Didier Barth avec the "Marais-Rouge" cooperative for providing the monitoring data and technical information of the heating plant as well as for his availability to answer their questions.

7. References

Bergman, T.L., Incropera, F.P., 2011. Fundamentals of heat and mass transfer. Wiley.

Haller, M., Perers, B., Bales, C., Paavilainen, J., Dalibard, A., Fischer, S., Bertram, E., 2013. TRNSYS Type 832 v5.01 „Dynamic Collector Model by Bengt Perers" - Updated Input-Output Reference. Rapperswil.

Haller, M.Y., Paavilainen, J., Konersmann, L., Haberl, R., Dröscher, A., Frank, E., Bales, C., Streicher, W., 2011. A unified model for the simulation of oil, gas and biomass space heating boilers for energy estimating purposes. Part I: Model development. J. Build. Perform. Simul. 4, 1–18. https://doi.org/10.1080/19401491003671944

Klein, S.A., Al., 2014. TRNSYS 17: A Transient System Simulation Program.

Lund, H., Werner, S., Wiltshire, R., Svendsen, S., Thorsen, J.E., Hvelplund, F., Mathiesen, B.V., 2014. 4th Generation District Heating (4GDH): Integrating smart thermal grids into future sustainable energy systems. Energy 68, 1–11. https://doi.org/10.1016/J.ENERGY.2014.02.089

Ruesch, F., 2020. BioSolFer Integration von Solarwärme in Biomasse Fernwärmenetze.

Sveinbjörnsson, D., Linn Laurberg Jensen, Trier, D., Bava, F., Hassine, I. Ben, Jobard, X., 2017. FLEXYNETS D2.3 - Large Storage Systems for DHC Networks.

Tschopp, D., Tian, Z., Berberich, M., Fan, J., Perers, B., Furbo, S., 2020. Large-scale solar thermal systems in leading countries: A review and comparative study of Denmark, China, Germany and Austria. Appl. Energy 270, 114997. https://doi.org/10.1016/j.apenergy.2020.114997

8. Nomenclature

Abbreviations	Description
DH	District Heating
fg	Flue gas
SF	Solar Fraction
loss	Heat losses

symbol	description	Unit
$\boldsymbol{\eta}$	Effiency	-
cvRMSE	Coefficient of variance of RMSE:	-
$\boldsymbol{\dot{Q}}$	Heat flow rate	kW
$\mathbf{Q_{sol}}$	Heat flow supplied by the solar system (storage output)	kWh
$\mathbf{Q_{boi}}$	Heat flow supplied by the wood boiler	kWh
$\mathbf{Q_{con}}$	Heat flow supplied by the flue gas condenser	kWh
U	Overall heat loss coefficient of the storage	$W/(m^2.K)$
VS	Storage volume	m^3
$\mathbf{VS_{spe}}$	Specific storage volume according to the gross area of the solar field	m^3/m^2